AFRL-RX-WP-TM-2014-0040

MODELING AND EVALUATING THE ENVIRONMENTAL DEGRADATION OF UHTCs UNDER HYPERSONIC FLOW (PREPRINT)

M.K. Cinibulk
AFRL/RXCC

T.A. Parthasarathy
UES, Inc.

M. Opeka
Naval Surface Warfare Center

FEBRUARY 2014
Final Report

AIR FORCE RESEARCH LABORATORY
MATERIALS AND MANUFACTURING DIRECTORATE
WRIGHT-PATTERSON AIR FORCE BASE, OH 45433-7750
AIR FORCE MATERIEL COMMAND
UNITED STATES AIR FORCE

NOTICE AND SIGNATURE PAGE

Using Government drawings, specifications, or other data included in this document for any purpose other than Government procurement does not in any way obligate the U.S. Government. The fact that the Government formulated or supplied the drawings, specifications, or other data does not license the holder or any other person or corporation; or convey any rights or permission to manufacture, use, or sell any patented invention that may relate to them.

This report was cleared for public release by the USAF 88th Air Base Wing (88 ABW) Public Affairs Office (PAO) and is available to the general public, including foreign nationals.

Copies may be obtained from the Defense Technical Information Center (DTIC) (http://www.dtic.mil).

AFRL-RX-WP-TM-2014-0040 HAS BEEN REVIEWED AND IS APPROVED FOR PUBLICATION IN ACCORDANCE WITH ASSIGNED DISTRIBUTION STATEMENT.

//Signature//

RANDALL S. HAY, Project Engineer
Composites Branch
Structural Materials Division

//Signature//

DONNA L. BALLARD, Deputy Chief
Composites Branch
Structural Materials Division

//Signature//

ROBERT T. MARSHALL, Deputy Chief
Structural Materials Division
Materials and Manufacturing Directorate

This report is published in the interest of scientific and technical information exchange, and its publication does not constitute the Government's approval or disapproval of its ideas or findings.

	Form Approved OMB No. 074-0188

1. REPORT DATE (DD-MM-YYYY)	2. REPORT TYPE	3. DATES COVERED *(From – To)*
February 2014	Final	06 November 2009- 01 January 2014

4. TITLE AND SUBTITLE
Modeling and Evaluating the Environmental Degradation of UHTCs under Hypersonic Flow (Preprint)

5a. CONTRACT NUMBER
In-house

5b. GRANT NUMBER

5c. PROGRAM ELEMENT NUMBER
62102F

6. AUTHOR(S)
(see back)

5d. PROJECT NUMBER
4347

5e. TASK NUMBER

5f. WORK UNIT NUMBER
X06L

7. PERFORMING ORGANIZATION NAME(S) AND ADDRESS(ES)
(see back)

8. PERFORMING ORGANIZATION REPORT NUMBER

9. SPONSORING / MONITORING AGENCY NAME(S) AND ADDRESS(ES)
Air Force Research Laboratory
Materials and Manufacturing Directorate
Wright-Patterson Air Force Base, OH 45433-7750
Air Force Materiel Command
United States Air Force

10. SPONSOR/MONITOR'S ACRONYM(S)
AFRL/RXCC

11. SPONSOR/MONITOR'S REPORT NUMBER(S)
AFRL-RX-WP-TM-2014-0040

12. DISTRIBUTION / AVAILABILITY STATEMENT
Approved for public release; distribution unlimited.

13. SUPPLEMENTARY NOTES
PA Case Number: 88ABW-2013-2417; Clearance Date: 28 May 2013. Journal article to be published in *Ultra-High Temperature Ceramics: Materials for Extreme Environment Applications*. This is a work of the U.S. Government and is not subject to copyright protection in the United States. Report contains color.

14. ABSTRACT
Recent advances in understanding the mechanisms of degradation of Ultra-High Temperature Ceramics (UHTCs) under hypersonic flight conditions are reviewed. Experimental and modeling efforts using leading edge samples of HfB2-20% (vol) SiC within a scramjet rig are presented. Other experimental efforts to study the behavior of UHTCs under simulated hypersonic conditions are reviewed.

15. SUBJECT TERMS
modeling, evaluation, UHTC degradation, hypersonic flow

16. SECURITY CLASSIFICATION OF:			17. LIMITATION OF ABSTRACT	18. NUMBER OF PAGES	19a. NAME OF RESPONSIBLE PERSON (Monitor)
a. REPORT	b. ABSTRACT	c. THIS PAGE			Randall S. Hay
Unclassified	Unclassified	Unclassified	SAR	52	19b. TELEPHONE NUBER *(include area code)* (937) 255-9825

REPORT DOCUMENTATION PAGE Cont'd

6. AUTHOR(S)

M.K. Cinibulk, AFRL/RXCC

T.A. Parthasarathy, UES, Inc.

M. Opeka, Naval Surface Warfare Center

7. PERFORMING ORGANIZATION NAME(S) AND ADDRESS(ES)

AFRL/RXCC
Air Force Research Laboratory
Materials and Manufacturing Directorate
Wright-Patterson Air Force Base OH 45433-7750

UES, Inc.
4401 Dayton Xenia Road
Dayton OH 45432

Naval Surface Warfare Center
Carderock, MD 20817

Ultra-High Temperature Ceramics: Materials for Extreme Environment Applications, Edited by William G. Fahrenholtz, Eric J. Wuchina, William E. Lee, and Yanchun Zhou
ISBN 0-471-9781118700785

Chapter 11

Modeling and Evaluating the Environmental Degradation of UHTCs under Hypersonic Flow

T. A. Parthasarathy[1, 2], M. K. Cinibulk[1], M. Opeka[3]

[1]Air Force Research Laboratory,
Materials and Manufacturing Directorate,
Wright-Patterson AFB, OH 45433
[2] UES, Inc., Dayton OH 45432
[3]Naval Surface Warfare Center, Carderock, MD 20817

Corresponding Author Name : T. A. Parthasarathy
Corresponding Author Phone: 937-255-9809
Corresponding Author Email: Triplicane.parthasarathy@us.af.mil

Keywords: modeling, evaluation, UHTC degradation, hypersonic flow

Abstract: Recent advances in understanding the mechanisms of degradation of Ultra-High Temperature Ceramics (UHTCs) under hypersonic flight conditions are reviewed. Experimental and modeling efforts using leading edge samples of HfB_2-20%(vol)SiC within a scramjet rig are

presented. Other experimental efforts to study the behavior of UHTCs under simulated hypersonic conditions are reviewed.

11.1 Introduction

Over the past decade, there has been a growing interest worldwide in developing aircraft that can travel at or greater than Mach 6.[1] Several short duration flight tests by NASA and the U.S. Air Force have shown that a scramjet engine can be used to achieve aircraft speeds of Mach 5 to Mach 10.[2-4] Extending these concepts towards the development of a vehicle for reusable or sustained flight now awaits the development of novel materials that can handle the aerothermal conditions imposed on some of the critical parts.[5] The sharp leading edges of the vehicle and cowl at the engine inlet as well as the fuel injection struts in the combustion section of the scramjet engine are considered to be the critical components with anticipated material temperatures that could reach as high as 2000°C through aerothermal heating at Mach 8.[6] Both components are required by current design to have a geometrically sharp leading edge (762 μm or 30 mils radius of curvature) that must be retained, while bearing the extreme environment resulting from hypersonic flight. Both materials development and modeling activities towards such an application were carried out in the 1950s and 1960s.

The conditions experienced by a sharp body under hypersonic flow conditions was modeled and published by scientists at, and/or funded by, NASA.[7-12] Materials development and modeling efforts were pursued under Air Force funding by Kauffman *et al.*[13-17] Based on the promising results from prior research and the recent worldwide interest for hypersonic aircraft development, there has been a renewed effort in research and development of ultra-high temperature ceramics (UHTCs), which are typically defined as non-oxide ceramics with chemical and structural stability above 2000°C.[18] It is now widely recognized that environmental degradation, and especially oxidation, under hypersonic flow conditions is the key life limiting factor for leading edge applications.[18-21] Thus, studying the oxidation kinetics and tailoring compositions to improve oxidation resistance have been the focus of the most recent work.

The most studied UHTC compositions are diborides of hafnium and zirconium with additives to control grain growth and/or improve oxidation resistance, the most common being SiC. The environmental response, especially oxidation, has been evaluated using several different methods. The most common has been the measurement of oxidation kinetics in a furnace atmosphere under isothermal conditions.[18; 22-31] Methods which also impose realistically high heating rates include arcjet testing[32; 33], laser-based heating [34] , electric heating [35; 36] or oxy-acetylene torch testing[37], and exposure inside a direct-

connect scramjet engine [38] [39; 40]. Among these,the arcjet testing is the most widely used historically by the Air Force and NASA for simulating reentry conditions. However, none of the tests used to date, including the arcjet test, are known to reproduce the actual conditions that a leading edge material will experience during hypersonic flight. Key parameters that represent these conditions with respect to material survivability are heat flux, total or stagnation temperature, total or stagnation pressure, dynamic pressure, fluid velocity at the material surface, fluid composition, degree of dissociation of gaseous elements, and catalytic recombination at the material's surface. In addition, under realistic conditions, resistance to acoustic and mechanical vibrations and thermal shock will also be important. Most of the oxidation experiments described in the literature are conducted in a laboratory furnace, thus assigning the total temperature as the key parameter of interest by default; all other factors are ignored. The tests that use laser as a heating source focus on reproducing the appropriate heat flux, and in some cases include fluid flow. The arcjet test generally focuses on reproducing the heat flux, a significant fraction of which depends on catalytic recombination of gases, which itself varies with material surface chemistry and morphology. The scramjet rig reproduces several of the aerothermal conditions predicted to be experienced during free flight, but it uses gases that differ in chemistry from air, and the actual gas flow velocities are not sufficient to cause dissociation of gases behind the bow shock.

The lack of an accepted test to evaluate the suitability of a candidate material for hypersonic applications has necessitated the need to develop a model to interpret the experimental data from the various testing techniques. Such a model would then enable the prediction of performance in actual hypersonic environments. Advances towards this objective are presented in this chapter. Figure 1 is a schematic that summarizes the approach that has been taken to address this objective. Progress in environmental modeling efforts, their limitations, and possible future directions are discussed.

FIGURE 1

11.2 Oxidation Modeling

The ideal model for oxidation kinetics of UHTCs will be one that is able to include all the control parameters of the experiments as input and predict any of the various parameters measured as outcome of the experiments. Further, the model will be able to translate data across different testing techniques and use them to predict performance in an actual application. Thermodynamic modeling of the oxidation process is the natural starting point in the development of such a model, since it will involve the least assumptions and could be considered as modeling from first principles. It also provides information on key chemical species that will clearly guide the modeling of the kinetics. In the literature,

relatively simple yet elegant oxidation kinetics models have been identified, such as the classic parabolic scale growth model formulated by Wagner with or without accounting for evaporation of scale at the surface.[41; 42] But the UHTCs have been found to form a complex scale which is heterogeneous and this defies simple models. In particular, the complex morphology, chemical composition and nature of the scale formation requires modifications to the Wagner model. Further, parameters that affect the kinetics require material properties that are not readily available or known with certainty. Thus oxidation kinetics modeling of UHTCs can be expected to include approximations. Given these difficulties, it is best to think of the resulting model as a methodology to interpret data rather than one derived from first principles. A large database is useful and fortunately, there is a large body of oxidation data is available in the literature from the 1960's as already mentioned, which we describe briefly before presenting modeling concepts.

The oxidation behavior of transition metal diboride-based UTHCs have been measured using a variety of methods and approaches. The earliest research identified the diborides of zirconium and hafnium as the best performers with respect to oxidation in flowing air at temperatures above 1600°C.[13; 15; 16] Later studies included composition modifications which resulted in the conclusion that HfB_2-20%volSiC was the most oxidation resistant at the highest temperatures. These studies utilized furnaces, forced flow air heaters and arc

heaters.[17; 43] This early research also included tests on leading edge geometries of candidate materials using arc heaters.[44] These were followed by more careful studies in air or Argon-oxygen mixtures in furnaces as well as thermo-gravimetric apparatus (TGA).[22] Typically, these evaluations reported scale thicknesses and sometimes recession rates, while TGA studies reported weight gain and weight of oxygen consumed as a function of time and temperature.

Oxidation studies on the most promising diborides were reinitiated in the 1990's. [26; 31] Much of the data reported on oxidation kinetics since then has been on the zirconium and hafnium diborides with SiC and other additions.[18; 26; 30; 45-47] The first modeling efforts were undertaken by Opeka[18] and Fahrenholtz[48; 49]. Opeka derived condensed/vapor phase equilibrium diagrams for the Zr-O, Si-O, and B-O systems at 2227°C, and assembled them to gain a thermodynamics-based description of the oxidation of the ZrB_2+SiC composition, which provided insight into the synergistic benefit of each oxide in the multi-component scale. While pure SiO_2-scale forming materials (eg., SiC) are limited to an approximately 1800°C usage due to the onset of active oxidation, the invariant vapor pressure of B_2O_3 with pO_2 was proposed to play a significant role by mitigating the active oxidation of the SiO_2-forming component above this temperature This study was followed by the work of Fahrenholtz who derived the volatility diagrams for ZrB_2 at 1000 K, 1800 K and 2500 K[49] with the P_{O2} calculated for the equilibrium co-existence of ZrB_2, ZrO_2 and B_2O_3, in contrast

with the unit activities assumed by Opeka. His work provided an expanded thermodynamics-based description of the Zr-O and B-O condensed/vapor phase reactions and associated vapor pressures as a function of the three selected temperatures (1000K, 1800K, 2500K) , and showed that B_2O_3(g) was the favored gaseous species at temperatures and pressures of engineering interest (Figure 2a). He further provided a temperature-dependent, vapor pressure-based description of the B-O system to gain insight into the weight fraction of liquid B_2O_3 retained in the condensed but porous ZrO_2 scale. The retained B_2O_3 was also experimentally determined by Talmy et al.[50] and her results shown reproduced in Figs. 2b (graphically) and 2c (microstructurally). Fahrenholtz expanded the thermodynamics-based analysis to the ZrB_2-SiC UHTC composition and proposed a reaction sequence for the oxidation process, associated scale composition and growth, and formation of a depleted zone of the SiC phase in the base ceramic [20]. These largely thermodynamics-based efforts were followed by the development of an oxidation kinetics model of these refractory diboride UHTCs by Parthasarathy *et al.*[51-53]

FIGURE 2

The initial modeling effort on the pure diborides of Zr and Hf by Parthasarathy *et al.* was based on a schematic representation of the experimentally observed microstructural observations, as shown in Fig. 3.[52] The model assumed that the scale is made of two regions, an external glassy layer of liquid boria and an internal region consisting of two phases, a solid, but porous oxide of zirconia (or hafnia) with the pores filled with liquid boria. The model assumed that the solid oxide phase was impermeable to oxygen based on prior experimental observations of very low electronic conductivity which would be required to ensure ambipolar diffusion where the transport of positively charged oxygen vacancies are accompanied by an appropriate (neutralizing) current of holes/electrons. The porous channels within the solid oxide were taken to be continuous and open such that oxygen can permeate through these channels to the substrate and oxidizes it. The oxygen permeation will be through a liquid of boria if the pores are filled, which happens at low temperatures. The molar ratio of boria to oxide formed from oxidation was taken to be proportional to the stoichiometry of the substrate diboride. Since the solid oxide was occupying most of the volume of the inner region, excess boria must be expelled as an external glassy layer (Fig. 3b). At the surface of this external boria layer, boria could evaporate by diffusion across a gaseous boundary layer whose width is determined by the flow conditions imposed. At intermediate temperatures the evaporation of boria is sufficiently fast that no external layer forms, and in fact

some boria from within the oxide pores evaporates leaving behind a partially porous oxide scale. Thus in the intermediate temperature regime, the oxygen permeates partially through these pores by gaseous diffusion or Knudsen diffusion and then through the remaining depth by permeation in liquid boria, as illustrated in Fig. 3a. At very high temperatures the boria is essentially lost by evaporation as rapidly as it forms, Fig. 3c. Using literature values for oxygen permeability and vapor pressures for boria, the model was able to capture oxidation data reported in the literature. In particular the model predicted the temperatures of the transitions as shown in Fig. 3d, in close agreement with experimental observations.

FIGURE 3

A key complication in both measuring and predicting oxidation kinetics of the refractory diborides is the fact that the oxidation product, boria, is a glass with rapidly decreasing viscosity with increasing temperature. At temperatures of engineering interest, which are 1200-1600°C, the boria viscosity is sufficiently low to cause it to flow under gravity.[54] Thus oxidized samples will show significant variation in glass thickness depending on the orientation of the surface.[23] These effects were included in a modified version of the model for oxidation of diborides.[51] In this model, the effect of fluid flow was taken into account using a model adapted from models of water flooding from rainfall. As

liquid boria forms by oxidation it is added to the surface while gravitational forces tend to drain the glass in inverse proportion to its viscosity. The differential rate determines the actual thickness that is measured at the end of the experiment. This effect dominates in the low temperature regime where boria forms an external layer, but is not a factor once boria recedes into the porous oxide scale due to evaporation.

In the final iteration of the model for diboride oxidation kinetics, two more assumptions of the prior model were relaxed. First, inclusion of the effect of volume change associated with monoclinic to tetragonal phase change of the MeO_2 phases is found to rationalize the observations by several investigators of abrupt changes in weight gain, recession, and oxygen consumed, as the temperature is raised through the phase transformation temperatures for ZrO_2 and HfO_2. Second, the inclusion of oxygen permeability in ZrO_2 is found to rationalize the enhancement in oxidation behavior at very high temperatures (>1800°C) of ZrB_2, while the effect of oxygen permeability in HfO_2 is negligible. An important outcome of this model was that the pore fraction of the HfO_2 and ZrO_2 selected (0.03 and 0.04 respectively) to rationalize the data was very close to the volumetric shrinkage associated with the phase transformations of HfO_2 and ZrO_2 from monoclinic to tetragonal. Based on these considerations, the significant advantage of HfB_2 over ZrB_2 was credited to the higher transformation temperature and lower oxygen permeability of HfO_2 compared with ZrO_2. As

shown in Fig. 4, the model can rationalize the observed behavior both with respect to recession and with respect to oxygen consumed simultaneously. The inclusion of the effect of dopants (impurities) in ZrO_2 or HfO_2 can rationalize the enhanced oxidation rates seen at the highest temperatures. This arises from the enhanced electronic conductivity of the oxides by permitting ambipolar oxygen transport.[52; 53; 55] At the highest temperatures of the tests, it is possible that the oxide scales become contaminated by impurities from the furnace itself. Such observations have been made by Carney et al. and reported in recent work, where significant amount of calcium was found in samples oxidized at the highest temperatures.[56] Finally, the model included the effect of oxygen partial pressure through the dependence of permeability in glass and pores on the oxygen partial pressure, and was able to rationalize the limited data available reasonably well, as shown in Fig 5.

FIGURE 4

FIGURE 5

The model for pure diboride oxidation was later extended to include SiC-containing compositions.[57] In this work, once again the modeling started with

the recognition of the oxidation product morphology and chemistry as shown in Fig. 6. Opila et al. first reported on the observation of a SiC-depleted zone beneath the substrate/oxide interface, during oxidation of ZrB_2- SiC.[20; 31] This phenomenon was confirmed and rationalized using thermodynamic modeling by Fahrenholtz.[20] As shown in Figure 7, thermodynamic calculations provided justification for the formation of a depleted zone. The kinetic modeling by Parthasarathy *et al*.[57] started with a reduction of the reported microstructures to a schematic representation (Fig. 8) superimposed with reactions known from prior thermodynamic modeling by Fahrenholtz.[20] The key conclusion of Fahrenholtz was that the internal depletion zone was due to internal active oxidation of SiC to SiO. The extension of this required a transport mechanism that is able to transfer oxygen fast enough to cause SiC oxidation faster than the oxidation rate of ZrB_2. This was achieved in the work of Parthasarathy *et al*.[57] by proposing a CO/CO_2 countercurrent mechanism, as had been derived earlier by Holcomb and St. Pierre.[58] The rest of the modeling involved including the effect of silica on the viscosity and oxygen permeability of the glassy region. These values are available in the literature for pure boria and silica, and some but not all intermediate compositions. The actual composition of borosilicate glass in the oxidation product is difficult to determine due to difficulties in measuring B content. The model assumed that the composition is the same as what might be predicted from stoichiometry of reactants and products and the volume fraction of the phases in

the substrate. The viscosity and permeability for this composition was in turn estimated by assuming a logarithmic mean as the composition varied from pure boria to pure silica. With these assumptions the model was able to capture the effect of SiC addition on the oxidation kinetics of ZrB_2- SiC as shown in Fig 9. The model was also able to capture kinetics of oxidation of HfB_2- SiC. It was found that the weight gain, and scale thicknesses were captured well, except at the highest temperatures. The depletion zone thickness is predicted to be significant (>1 μm in 2.5 h) at temperatures above 1550°C. The experimentally observed depletion zone thicknesses are sometimes significantly larger than that predicted, implying an effect not yet captured by the model.

FIGURE 6

FIGURE 7

FIGURE 8

FIGURE 9

11.3 UHTC LE Behavior under Simulated Hypersonic Conditions

The application of UHTC compositions is at present focused on the cowl leading edge and fuel injection struts of scramjet engine for hypersonic flight. These two applications involve a unique geometry, thermal loading with large temperature gradients, very high fluid velocities with its associated mechanical vibrations, aerodynamic and aerothermal loads. While there are a number of tests that have evolved over the past several decades as mentioned in the introduction, this section focuses on a recent study that examined the use of a direct-connect scramjet engine as a wind tunnel to simulate conditions of free flight of leading edge samples of a UHTC (HfB_2-20%volSiC) composition.

The details of the purpose, design, construction and evaluation of the direct-connect scramjet engine have been described by Gruber *et al*.[38; 59; 60] A brief description is given here. Ambient air is compressed before being expanded through an isolator nozzle resulting in a supersonic flow at Mach 1.8 to

2. The cooling that results from the expansion is augmented by adding heat using a combustion heater. The oxygen lost during combustion heating, is compensated for by adding oxygen to ensure the correct partial pressure of oxygen in the resulting fluid that enters the supersonic combustor. The post combustion section employs an exit nozzle before reaching a probe housing. It is within the probe housing that leading edge samples were introduced. The gas composition at this location varies with combustor section but typically includes 5-10% moisture with a total static pressure near 1 atm. The samples were mounted on a sample holder, constructed of water-cooled thermal barrier-coated Inconel.[39; 40] The samples were visible during the run through quartz windows. The scramjet rig was fully calibrated and all important parameters including enthalpy, total temperatures, gas flow velocities, gas composition, and pressures were available as a function of time during the run. The fluid flow parameters such as velocity (U) and static pressure (p_1), along with static temperature (T_1) and specific heat ratio of the gas composition (γ) were used to calculate the heat flux (Q_w) experienced by the leading edge samples.[7; 10]

$$M = U / \sqrt{\gamma R T_1} \quad \ldots (1)$$

$$T_t = T_1\left(1+\frac{\gamma-1}{2}M^2\right) \quad \ldots (2)$$

$$p_{t2} = p_1\left(\frac{\gamma+1}{2}\right)^{\frac{\gamma}{\gamma-1}}\left(\frac{(\gamma+1)M^2}{2\gamma M^2-(\gamma-1)}\right)^{\frac{1}{\gamma-1}} M^2 \quad \ldots (3)$$

$$(h_{aw} - h_w), kJ/kg = C_p(T_t - T_{wall}) \quad \ldots (4)$$

$$\dot{Q}_w, W/m^2 = 3.88x10^{-4}\sqrt{\frac{p_{t2}(Pa)}{r(m)}}(h_{aw} - h_w) \quad \ldots (5)$$

In the above set of equations, M is the Mach number, T_t is the total temperature, T_{wall} the material surface temperature, p_{t2} is the total pressure behind the bow shock, r is the radius of curvature of the leading edge, C_p the specific heat of fluid, h_{aw} is the total enthalpy of the fluid ($=C_pT_t$), the h_w the enthalpy of the fluid at the material wall temperature ($=C_pT_{wall}$). The heat flux varies with orientation of the material wall as well as distance form the bow shock. These variations are given by the following.

$$\dot{Q}(\theta) = \dot{Q}_w \, \mathbf{Cos(}\theta\mathbf{)} \quad \ldots (6)$$

$$\dot{Q}(x) = \dot{Q}_w Cos(\theta_c)/\sqrt{x} \quad \ldots (7)$$

Where θ gives the angle between the direction of fluid flow and the normal to the wall surface (=0 at the tip of the leading edge), and x is the distance from the tip of the leading edge. θ_c and Q_w refer to the orientation and the heat flux at the tangential point where the cylindrical surface of the tip meets the slant face of the leading edge wedge. It must be noted that while the Equations (6) and (7) capture the dependences accurately, they are approximations to the actual variation of the heat flux. Further note that the net heat flux at any location is a function of the wall temperature and thus will vary with time. The steady state material

temperature will depend on radiation heat flux back to the atmosphere and thermal conduction within the solid. The wall temperature will depend on the static temperature of the fluid and material thermal properties. Thus a thermal model that includes the aerothermal heating, radiation and conduction for a given geometry is required. Using such a model, the thermal profiles were calculated for a large (50.8 x 50.8mm) leading edge sample under free flight and compared to the thermal response of a smaller (12.7 mm x 12.7mm) leading edge sample used in the scramjet rig.[40] The results from these calculations are shown reproduced in Fig. 10. An important outcome of the thermal model was that the thermal properties of the material significantly affect the temperature gradient. Materials based on diboride UHTCs have higher thermal conductivities at high temperatures than other ceramics including SiC, potentially making them better material candidates for these applications.

FIGURE 10

Figure 11 shows a typical oxidation scale formed on a UHTC (HfB_2-20vol%SiC) leading edge sample after exposure in the scramjet. The microstructural characterization of the UHTC showed that the scale was different than what is normally observed in samples after furnace oxidation. First, the

external glassy layer is absent. Second, no depletion layer was observed. Third, silica was absent in the outer regions of the hafnium rich oxide scale. Fourth, the formation of hafnon ($HfSiO_4$) was observed in the outer regions. While the reasons for these differences are not clear, it is suspected that the high flow rate of the environment along with the presence of moisture in the atmosphere may be responsible for these differences.

FIGURE 11

11.4 Comparing Model Predictions to Leading Edge Behavior

The modeling work by Parthasarathy *et al*.[57] included the effect of fluid flow on the evaporation rates of boria and silica and thus was considered sufficient for predicting the behavior of the leading edges exposed to simulated hypersonic conditions. The model however did not include the physical shear mechanism by which the external glassy layer could be thinned down. Under most conditions of the test the evaporation rates were high enough to result in little or no external glassy layer; thus the shear forces were irrelevant. The thermal model described in the earlier section was used to obtain the thermal profile (time vs temperature) at the tip of the leading edge and fed into the oxidation model to predict the oxidation scale thickness, depletion thickness, and recession. The

aerothermal calculations were used to obtain the total pressure and fluid velocity behind the bow shock and used for the model predictions. The results obtained showed that he predicted oxide thicknesses were close to the experimental data, although they were consistently lower. Impurities and moisture in the environment could have altered the oxygen permeation across the scales. The formation of hafnon could have increased the volume fraction of the porous channels. Finally, the possibility of glassy material being drawn out of the porous channels by the high velocity fluid flow was suggested.

Based on the reasonable predictions presented above, the model was used to estimate the behavior of a UHTC leading edge behavior under hypersonic free flight conditions. Figure 12 summarizes the predictions. The results are shown as a function of free flight Mach numbers. The leading edge tip temperatures, steady state heat flux, thermal gradients in the sample, and oxidation thickness with time are shown. It must be noted that the results are sensitive to the thermal conductivity and specific heat of the composition used. There is a significant variation in thermal properties of UHTCs with processing method as has been noted by several groups.[32] For example, the use of SiC will result in higher tip temperatures due to the lower thermal conductivity at high temperatures, when compared with UHTCs.

FIGURE 12

In closing, the following limitations are worth pointing out with a view to direct future work. The oxidation modeling of UHTCs includes some assumptions that are discussed below. First the refractory oxide, ZrO_2 or HfO_2, is assumed to be impermeable to oxygen due to low electronic conductivity. This is a good approximation if the oxide is pure, but impurities can enhance the conductivity significantly especially at high temperatures (>2000K). The impurities may be present in the raw materials or may be acquired during testing or use. Second, the variation of boria content with distance in the scale has been approximated, and boria content can significantly affect viscosity and oxygen permeation in borosilicate glasses. Third the effect of mechanical shear on the external glassy layer has been ignored.

The scramjet rig offers a unique approach to evaluate LE candidate materials using simulated hypersonic conditions, but there are some limitations. First, the gas chemistry is not that of ambient air. The gas contains a significant amount of water and carbon-dioxide (about 10% each). In addition impurities from the components of the rig cannot be easily avoided. The use of water as coolant for parts of the rig interfered with observation as it collected in the recess of the window; however future design changes could alleviate this. The glass windows currently in use prevented the use of optical pyrometry. The use of a suitable material such as ZnSe for the window will alleviate this difficulty

provided the material is stable at the temperatures of the rig walls. The actual velocity of the gases is not hypersonic even though the heat content of the gases simulates hypersonic flight conditions. The rig used in the reported work is limited to a maximum of Mach 7. Finally, the scramjet rig is a unique facility available only to a very limited group of researchers and only at periodic intervals. However if the community recognizes it to be a useful method, a dedicated rig might be constructed that is smaller in scale, but it will not be inexpensive.

11.5 Behavior of UHTCs under other Test Methods

Various compositions of UHTCs are being studied by different investigators to explore the possibility of enhancing the environmental degradation resistance at high temperatures. The evaluation has largely been based on furnace oxidation tests due to the ease and low cost of the test method. It is appropriate for initial screening of compositions and for understanding mechanisms of oxidation in static laboratory air; however using these data to predict performance under hypersonic flight conditions is not trivial. Using a mechanistic model that captures the furnace data in combination with scramjet exposure tests, shows promise. In the literature, one can find several other approaches that have been pursued to evaluate performance of candidate materials

for thermal protection under hypersonic flight conditions. The merits and demerits of these approaches are discussed briefly below.

Arcjet Test

The arcjet test is a widely accepted method for evaluating performance of materials under re-entry conditions, developed and used widely by NASA to design space vehicles. It uses a plasma generated gas mixture which contains a high fraction of ionized atoms of oxygen and nitrogen. Recombination of the charged species is catalyzed by the sample surface to release heat. The plasma is accelerated to high velocities (supersonic but not hypersonic) using an electric field before it is directed on to the sample. The enthalpy of the gases per unit area of the sample is reported as well as the surface temperature of the sample which is measured using an optical pyrometer. The key advantage of this method is that it provides a simulation of dissociation of air that occurs behind the bow shock at hypersonic speeds. The catalytic coefficient for recombination varies with sample composition and can also change during the test since the surface composition changes as the sample oxidizes complicating interpretation and modeling of the test results. Until recently the test has used mostly flat samples or large radius conical samples, thus the effect of a sharp leading edge geometry had not yet been captured in the test. Recent works are beginning to study samples with sharp geometry, but the aerothermal heat flux distribution during free flight is not reproduced in these tests.[61-63] The test is also not best for evaluating materials

for hypersonic speeds in the range of Mach 5 to 7, where there is very little dissociation of gases expected. Finally the very high cost of the test makes it prohibitive for most studies.

Laser Test

The availability of laser facilities at reasonable cost compared to arcjets has resulted in tests that evaluate UHTC compositions using lasers as the heat source. These tests use a prescribed heat flux, calibrated using optical standards, on a flat geometry of the sample for a predetermined length of time. In some cases, an external tangential flow of air typically at subsonic speeds is included. The advantage of this method is that it requires a short set-up, run time, and several samples can be tested within a short period of time. The ambient fluid composition is nearly exact as it is air and material surface temperature can be monitored accurately during the test using optical pyrometry. The key disadvantage of the method is that the actual heat flux absorbed by the sample varies with the composition, the wavelength of the laser, and temperature of the sample. Thus the laser absorptance and emitance of each sample must be measured as a function of temperature and accounted for in interpreting the results. There are very few studies on these properties of UHTCs, with most studies assuming the absorptance to be unity. Emissivity has been reported in some recent work, but factors such as machining method can influence emissivity.[64; 65] The laser method also uses a constant heat flux, whereas in

real flight the heat flux varies from nearly the cold wall heat flux to the steady state heat flux gradually as the sample heats up. The steady state heat flux will be affected by the emissivity of the material and the ambient temperature during flight; this is not captured in the laser test.

Oxy-Acetylene Torch Test

The oxy-acetylene torch has long been used as a heat source, and has recently been revived as a low-cost alternative to arcjet and laser tests. In this test a flat sample is exposed to the hot combustion gases of an oxy-acetylene torch by holding the sample at a calibrated distance from the torch tip. The calibration is usually made based on the measured optical pyrometer reading on the hottest section of the exposed sample. The heat flux is usually not measured or reported. The advantages of this method is that it provides high heat fluxes, is very quick and inexpensive, and as such, can be used as an good oxidation screening tool for the relative comparison of material compositional variations. The disadvantage is the lack of standardization of the test procedure and lack of calibration with respect to heat flux. The exact composition of the combustion product is also unknown and depends on the initial oxygen-acetylene ratio, as well as on location within the flame. Water is present as a major product of combustion, which can complicate interpretation of the results.

11.6 Summary

The status of mechanistic understanding of the degradation of UHTC leading edge components under hypersonic flight conditions was reviewed. The oxidation behavior studied under conventional methods and reported over the past several decades could be interpreted reasonably well using analytical models that assume the glassy regions as the only pathway for oxygen permeation. Extension of this model to hypersonic flow conditions shows promise but more experimental and modeling work is required to develop a comprehensive understanding. UHTC-based leading edge samples appear to withstand the simulated hypersonic conditions up to Mach 7. However the UHTC is found to degrade much more rapidly under arcjet conditions. The behavior under arcjet appears to be unique and different from other test methods, and thus the least understood.

Figure Captions

Figure 1

Overview of the approach used to model and evaluate UHTC leading edge materials under simulated hypersonic flow conditions by Parthasarathy *et al*. [39; 40; 51-53; 57]

Figure 2

(a) Thermodynamic model for the oxidation of ZrB_2 by Fahrenholtz [49] plotted in terms of phase stability regions for various stochiometric compounds. (b) Observation by Talmy *et al*. of the decrease in retained boria in the scale with temperature shown replotted using data[50] and (c) microstructural cross-section of ZrB_2 after oxidation at 1500°C in air for 30min, presented by Fahrenholtz.[49].

Figure 3

(a) A schematic of the microstructure interpreted from experimental data and used to build the oxidation model for ZrB_2. The loss of boria was taken to be limited by diffusion through porous channels in the intermediate temperature regime. (b) At lower temperatures an external liquid boria forms and remains stable (c) at very high temperatures the boria evaporates as fast as it can form leading to rapid oxidation. (d) The transition between the three regimes as a function of temperature as predicted by the model of Parthasarathy *et al*.[52]

Figure 4

The oxidation model of Parthasarathy et al. [53] was able to rationalize the sudden jumps in oxidation kinetics with temperature in the ZrB_2 and HfB_2 systems, by proposing that the volume change associated with phase transformation from monoclinic to tetragonal oxide (ZrO_2 or HfO_2) opens up the porous channels in the scale. At the highest temperatures, the possible effect of unintentional dopant on the electronic conductivity of the oxide and thus the oxidation kinetics was estimated and was found to correlate with experimental data.

Figure 5

The proposed oxidation model [52] appears to capture the effect of oxygen partial pressure, but the data in the literature are rather limited.

Figure 6

Microstructure and EDS mapping of the oxidation product of a 20 vol% SiC-containing ZrB_2 sample showing the phases present along with morphology and a depleted zone lacking SiC in a matrix of ZrB_2 after exposure in air at 1627°C for 100 min.[20; 31]

Figure 7

Thermodynamic model for the oxidation of ZrB_2-SiC calculated by Fahrenholtz [48]along with a schematic sketch showing a rationale for the formation of a depleted zone as observed by Opila et al. (Fig. 6).

Figure 8

A schematic of the microstructural morphology and phase content of the oxidation product extracted from experimental work (e.g., Fig. 6), used in the model of Parthasarathy et al.[57]

Figure 9

The predicted variation in oxidation kinetics of SiC-containing ZrB2 as a function of SiC content compared with experimental data of Talmy[66] and Wang et al.[67]. Figure reproduced from the work of Parthasarathy et al.[57]

Figure 10

The thermal model of a leading edge sample of UHTC was compared for two cases, one for the sample used in the scramjet tests and another simulating free flight in the application. The results showed that the thermal profiles are nearly the same for the two cases near the leading edge tip, which were of experimental interest.[40]

Figure 11

The oxidation scale formed on the UHTC sample tested in the scramjet under conditions representing free-flight Mach numbers of 6.2 to 7. No external glassy layer or depleted zone was observed; however, hafnon ($HfSiO_4$) was present in the oxide scale as evidenced by both X-ray diffraction and EPMA analysis shown here.[40]

Figure 12

The thermal model for the leading edge (made of HfB_2-20% vol SiC) under hypersonic flight when combined with the oxidation models can predict parameters of interest for design as shown here. The temperature at the tip of the leading edge is shown to be lower than the total temperature often assumed. Similarly, the steady state heat flux is lower than the cold wall heat flux. The thermal profiles show a steep drop in temperature away from the tip and the oxidation rates appear to be tolerable for UHTCs at Mach 6.5.[40]

References

1. T. A. Jackson, D. R. Eklund, and A. J. Fink, "High speed propulsion: Performance advantage of advanced materials," *J Mater. Sci.,* 39 5905-5913 (2004).
2. R. T. Voland, L. D. Huebner, and C. R. McClinton, "X-43A Hypersonic vehicle technology development," *Acta Astronautica,* 59 181-191 (2006).
3. S. Cook and U. Hueter, "NASA's Integrated Space Transportaion Plan - 3rd Generation Reusable Launch Vehicle Technology Update," *Acta Astronautica,* 53 719-728 (2003).
4. G. Norris, "High-Speed Strike Weapon To Build On X-51 Flight," *Aviation Week & Space Technology*[May 20] (2013).
5. C. R. McClinton, V. L. Rausch, R. J. Shaw, U. Metha, and C. Naftel, "Hyper-X:Foundation for future hypersonic launch vehicles," *Acta Astronautica,* 57 614-622 (2005).
6. R. J. Kerans, "Concurrent Material and Structural Design with Innovative Ceramic Composites," *Final Report for DARPA/DSO*[AFRL Tehc. Report : AFRL-ML-WP-TR-2006-4130] (2005).
7. AmesResearchStaff, "Equations, Tables and Charts for Compressible Flow," *National Advisory Committe for Aeronautics*[Report 1135] (1953).
8. L. Lees, "On the boundary layer equations in hypersonic flow and their approximate solutions," *J Aero. Sci.,* 20 [2] 143-145 (1953).
9. J. A. Fay and F. R. Riddell, "Theory of stagnation point heat transfer in dissociated air," *J Aero. Sci.,* 25 73-85 (1958).
10. E. V. Zoby, "Empirical stagnation-point heat-transfer relation in several gas mixtures at high enthalpy levels," *NASA tech note, NASA TN D-4799* (1968).
11. S. M. Scala and L. M. Gilbert, "Theory of hypersonic laminar stagnation region heat transfer in dissociating gases," *NASA tech note NAS 7-100* Accession No. N71-70918 (1963).
12. NASA, "U S Standard Atmosphere," *NOAA document ST 76-1562* (1976).

13. E. V. Clougherty, R. L. Pober, and L. Kaufman, "Synthesis of oxidation resistant metal diboride composites," *Trans. Met. Soc. AIME*, 242 1077-1082 (1968).
14. L. Kaufman and E. Clougherty, *Technical Report RTD-TDR-63-4096 : Part 1, AFML, WPAFB, OH*[Dec.] (1963).
15. L. Kaufman and E. Clougherty, "Investigation of boride compounds for very high temperature applications," *Technical Report RTD-TDR-63-4096 : Part 2, AFML, WPAFB, OH*[Feb.] (1965).
16. L. Kaufman, E. V. Clougherty, and J. B. Berkowitz-Mattuck, "Oxidation characteristics of Hafnium and Zirconium Diboride," *Transactions of Metall. Soc. of AIME*, 239 458-466 (1967).
17. L. Kaufman and H. Nesor, "Stability characterization of refractory materials under high velocity atmospheric flight conditions, Part III, Vol. III: Experimental results of high velocity hot gas/cold wall tests," *AFML-TR-69-84* (1970).
18. M. M. Opeka, I. G. Talmy, and J. A. Zaykoski, "Oxidation-based materials selection for 2000°C+ hypersonic aerosurfaces: Theoretical considerations and historical experience," *J. Mater. Sci.*, 39 5887-5904 (2004).
19. F. Montverde, R. Savino, and M. Fumo, "Dynamic oxidation of ultra-high temperature ZrB2–SiC under high enthalpy supersonic flows," *Corrosion science*, 53 922-929 (2011).
20. S. R. Levine, E. J. Opila, M. C. Halbig, J. D. Kiser, M. Singh, and J. A. Salem, "Evaluation of ultra-high temperature ceramics for aeropropulsion use," *Jl Eur. Ceram. Soc.*, 22 2757-2767 (2002).
21. J. Marschall, D. A. Pejakovic, W. G. Fahrenholtz, G. E. Hilmas, S. Zhu, J. Ridge, D. G. Fletcher, C. O. Asma, and J. Thomel, "Oxidation of ZrB2–SiC Ultrahigh-Temperature Ceramic Composites in Dissociated Air," *J Thermophysics and Heat Transfer*, 23 [2] 267-278 (2009).
22. W. C. Tripp and H. C. Graham, "Thermogravimetric study of the oxidation of ZrB2 in the temperature range of 800 to 1500 C," *J. Electrochem. Soc.*, 118 [7] 1195-1199 (1971).
23. C. M. Carney, P. Mogilevsky, and T. A. Parthasarathy, "Oxidation behavior of zirconium diboride silicon carbide produced by the spark plasma sintering method," *J Amer. Ceram. Soc.*, 92 [9] 2046-2052 (2009).
24. C. M. Carney, "Oxidation resistance of hafnium diboride-silicon carbide from 1400-2000C," *J Mater. Sci.*, 44 5673-5681 (2009).
25. C. M. Carney, T. A. Parthasarathy, and M. K. Cinibulk, "Oxidation Resistance of Hafnium Diboride Ceramics with Additions of Silicon Carbide and Tungsten Boride or Tungsten Carbide," *J. Amer. Ceram. Soc.*, 94 [8] 2600-2607 (2011).

26. M. M. Opeka, I. G. Talmy, E. J. Wuchina, J. A. Zaykoski, and S. J. Causey, "Mechanical, thermal and oxidation properties of refractory hafnium and zirconium compounds," *Jl. Eur. Ceram. Soc.,* 19 2405-2414 (1999).
27. S. Meng, H. Chen, J. Hu, and Z. Wang, "Radiative properties characterization of ZrB2–SiC-based ultrahigh temperature ceramic at high temperature," *Materials and Design,* 32 377-381 (2011).
28. X.-H. Zhang, P. Hu, and J.-C. Han, "Structure evolution of ZrB2-SiC during the oxidation in air," *J Mater. Res.,* 23 [7] 1961-1972 (2008).
29. W.-B. Han, P. Hu, X.-H. Zhang, J.-C. Han, and S.-H. Meng, "High-Temperature Oxidation at 19001C of ZrB2–xSiC Ultrahigh-Temperature Ceramic Composites," *J. Amer. Ceram. Soc.,* 91 [10] 3328-3334 (2008).
30. E. Opila, S. Levine, and J. Lorincz, "Oxidation of ZrB2- and HfB2-based ultra-high temperature ceramics: Effect of Ta additions," *J Mater. Sci.,* 39 5969-5977 (2004).
31. E. J. Opila and M. C. Halbig, "Oxidation of ZrB2-SiC," *Ceram. Eng. Sci. Proc.,* 22 [3] 221-228 (2001).
32. M. Gasch and S. Johnson, "Physical characterization and arcjet oxidation of hafnium-based ultra high temperature ceramics fabricated by hot pressing and field-assisted sintering," *Jl Eur Ceram. Soc.,* 30 2337-2344 (2010).
33. R. Savino, M. D. S. Fumo, D. Paterna, A. D. Maso, and F. Monteverde, "Arc-jet testing of ultra-high-temperature-ceramics," *Aerospace Science and Technology,* 14 178-187 (2010).
34. D. D. Jayaseelan, H. Jackson, E. Eakins, P. Brown, and W. E. Lee, "Laser modified microstructures in ZrB2, ZrB2/SiC and ZrC," *J Eur Ceram. Soc.,* 30 [11] 2279-2288 (2010).
35. S. N. Karlsdottir and J. W. Halloran, "Oxidation of ZrB2-SiC: Influence of SiC content on Solid and Liquid Oxide Phase Formation," *J. Amer. Ceram. Soc.,* 92 [2] 481-486 (2009).
36. S. Gangireddy, S. N. Karlsdottir, and J. W. Halloran, "High-Temperature Oxidation at 19001C of ZrB2–xSiC Ultrahigh-Temperature Ceramic Composites," *Key Engineering Materials,* 434-435 144-148 (2010).
37. A. Paul, D. D. Jayaseelan, S. Venugopal, E. Zapata-Solvas, J. Binner, B. Vaidhyanathan, A. Heaton, P. Brown, and W. E. Lee, "UHTC composites for hypersonic applications," *Bull. Am. Ceram. Soc.,,* 91 [1] 1-8 (2012).
38. M. Gruber, J. Donbar, K. J. Jackson, T. Mathur, R. Baurle, D. Eklund, and C. Smith, "Newly developed direct-connect high-enthalpy supersonic combustion research facility," *J Propulsion and Power,* 17 [6] 1296-1304 (2001).
39. T. A. Parthasarathy, M. D. Petry, G. Jefferson, M. K. Cinibulk, T. Mathur, and M. R. Gruber, "Development of a Test to Evaluate Aerothermal

Response of Materials to Hypersonic Flow Using a ScramjetWind Tunnel," *Int. J of Appl. Ceram. Tech.,* 8 [4] 832-847 (2011).
40. T. A. Parthasarathy, M. D. Petry, M. K. Cinibulk, T. Mathur, and M. R. Gruber, "Thermal and oxidation response of UHTC leading edge samples exposed to simulated hypersonic flight conditions," *J. Amer. Ceram. Soc.,* 96 [3] 907-915 (2013).
41. C. Wagner, "Theoretical Analysis of the Diffusion Processes Determining the Oxidation Rate of Alloys," *J. Electrochem. Soc.,* 99 [10] 369-380 (1952).
42. C. Wagner, "Passivity and inhibition during the oxidation of metals at elevated temperatures," *Corrosion Science,* 5 751-764 (1965).
43. J. R. Fenter, "Refractory diborides as engineering materials," *SAMPE Quarterly,* 2,3 [1-15] (1971).
44. M. L. Hill, "Materials for small radius leading edges for hypersonic vehicles," *AIAA/ASME conference on Structures, Structural dynamics and Materials* (1967).
45. F. Monteverde and A. Bellosi, "Oxidation of ZrB2-based ceramics in dry air," *J Electrochem.Soc.,* 150 [11] B552-559 (2003).
46. W. G. Fahrenholtz, G. E. Hilmas, A. L. Chamberlain, and J. W. Zimmermann, "Processing and characterization of ZrB2-based ultra-high temperature monolithic and fibrous monolithic ceramics," *Jl of Mater. Sci.,* 39 [19] 5951-5957 (2004).
47. E. Wuchina, M. Opeka, S. Causey, K. Buesking, J. Spain, A. Cull, J. Routbort, and F. Guitierrez-Mora, "Designing for ultrahigh-temperature applications: The mechanical and thermal properties of HfB2, HfCx, HfNx and a-Hf(N)," *J. Mater. Sci.,* 39 5939-5949 (2004).
48. W. G. Fahrenholtz, "Thermodynamic Analysis of ZrB2–SiC Oxidation: Formation of a SiC-Depleted Region," *J. Amer. Ceram. Soc.,* 90 [1] 143-148 (2007).
49. W. G. Fahrenholtz, "The ZrB2 volatility diagram," *J. Amer. Ceram. Soc.,* 88 [12] 3509-3512 (2005).
50. I. G. Talmy, J. A. Zaykoski, and M. A. Opeka, "Porperties of ceramics in the ZrB2/ZrC/SiC system prepared by reactive processing," *Ceram. Eng. Sci. Proc.,* 19 [3] (1998).
51. T. A. Parthasarathy, R. A. Rapp, M. Opeka, and R. J. Kerans, "A model for transitions in oxidation regimes of ZrB2," *Materials Science Forum,* Vols. 595-598 823-832 (2008).
52. T. A. Parthasarathy, R. A. Rapp, M. Opeka, and R. J. Kerans, "A model for the oxidaiton of ZrB2, HfB2 and TiB2," *Acta Mater.,* 55 5999-6010 (2007).
53. T. A. Parthasarathy, R. A. Rapp, M. Opeka, and R. J. Kerans, "Effect of Phase Change and Oxygen Permeability in Oxide Scales on Oxidation

Kinetics of ZrB2 and HfB2," *J Amer. Ceram. Soc.,* 92 [5] 1079-1086 (2009).
54. R. A. Eppler, "Viscosity of molten B2O3," *J Amer Ceram.Soc.,* 49 [12] 679-680 (1966).
55. J. W. Patterson, *J Electrochem.Soc.,* 118 1033-1039 (1971).
56. C. M. Carney, T. A. Parthasarathy, and M. K. Cinibulk, "Separating Test Artifacts from Material Behavior in the Oxidation Studies of HfB2–SiC at 2000°C and Above," *Int. J. Appl. Ceram. Technol.* (in press).
57. T. A. Parthasarathy, R. A. Rapp, M. Opeka, and M. K. Cinibulk, "Modeling Oxidation Kinetics of SiC-containing Refractory Diborides," *J Amer. Ceram. Soc.,* 95 [1] 338-349 (2012).
58. G. R. Holcomb and G. R. St.Pierre, "Application of a counter-current gaseous diffusion model to the oxidation of Hafnium carbide at 1200C to 153OC," *Oxidation of metals,* 40 [1/2] 109-118 (1993).
59. T. Mathur, M. Gruber, K. Jackson, J. Donbar, W. Donaldson, T. Jackson, and F. Billig, "Supersonic combustion experiments with a cavity-based fuel injector," *J Propulsion and Power*, 17 [6] 1305-1312 (2001).
60. M. Gruber, S. Smith, and T. Mathur, "Experimental Characterization of Hydrocarbon-Fueled Axisymmetric Scramjet Combustor Flowpaths," *AIAA Paper 2011-2311* (2011).
61. L. Scatteia, D. Alfano, S. Cantoni, F. Monteverde, M. D. S. Fumo, and A. D. Maso, "Plasma Torch Test of an Ultra-High-Temperature Ceramics Nose Cone DemonstratoR," *Journal of Spacecraft and Rockets,* 47 271-279 (2010).
62. R. Gardi, A. D. Vecchio, G. Marino, and G. Russo, "CIRA activities on UHTC's: on-ground and in flight experimentations," *Proc. of 17th AIAA International Space Planes and Hypersonic Systems and Technologies,* Paper 2011-2303 (2011).
63. F. Monteverde, D. Alfano, and R. Savino, "Effects of LaB6 addition on arc-jet convectively heated SiC-containing ZrB2-based ultra-high temperature ceramics in high enthalpy supersonic air-flows," *Corrosion science* (in press).
64. L. Scatteia, D. Alfano, F. Monteverde, J.-L. Sans, and M. Balat-Pichelin, "Effect of the Machining Method on the Catalycity and Emissivity of ZrB2 and ZrB2–HfB2-Based Ceramics," *Jl of Amer. Ceram. Soc.,* 91 1461-1468 (2008).
65. L. Scatteia, R. Borrelli, G. Cosentino, E. Beche, J.-L. Sans, and M. Balat-Pichelin, "Catalytic and radiative behaviors of ZrB2-SiC ultrahigh temperature ceramic composites," *Journal of Spacecraft and Rockets,* 43 1004-1012 (2006).

66. I. Talmy, "Effect of SiC content on oxidation kinetics of SiC-ZrB2," *Unpublished work, Naval Surface Warfare Center, Carderock, MD* (2005).
67. M. Wang, C.-A. Wang, L. Yu, Y. Huang, and Z. Zhang, "Oxidation behavior of SiC platelet-reinforced ZrB2 ceramic matrix composites," *International J. App. Ceram. Tech.*, 9 [1] 178-185 (2012).

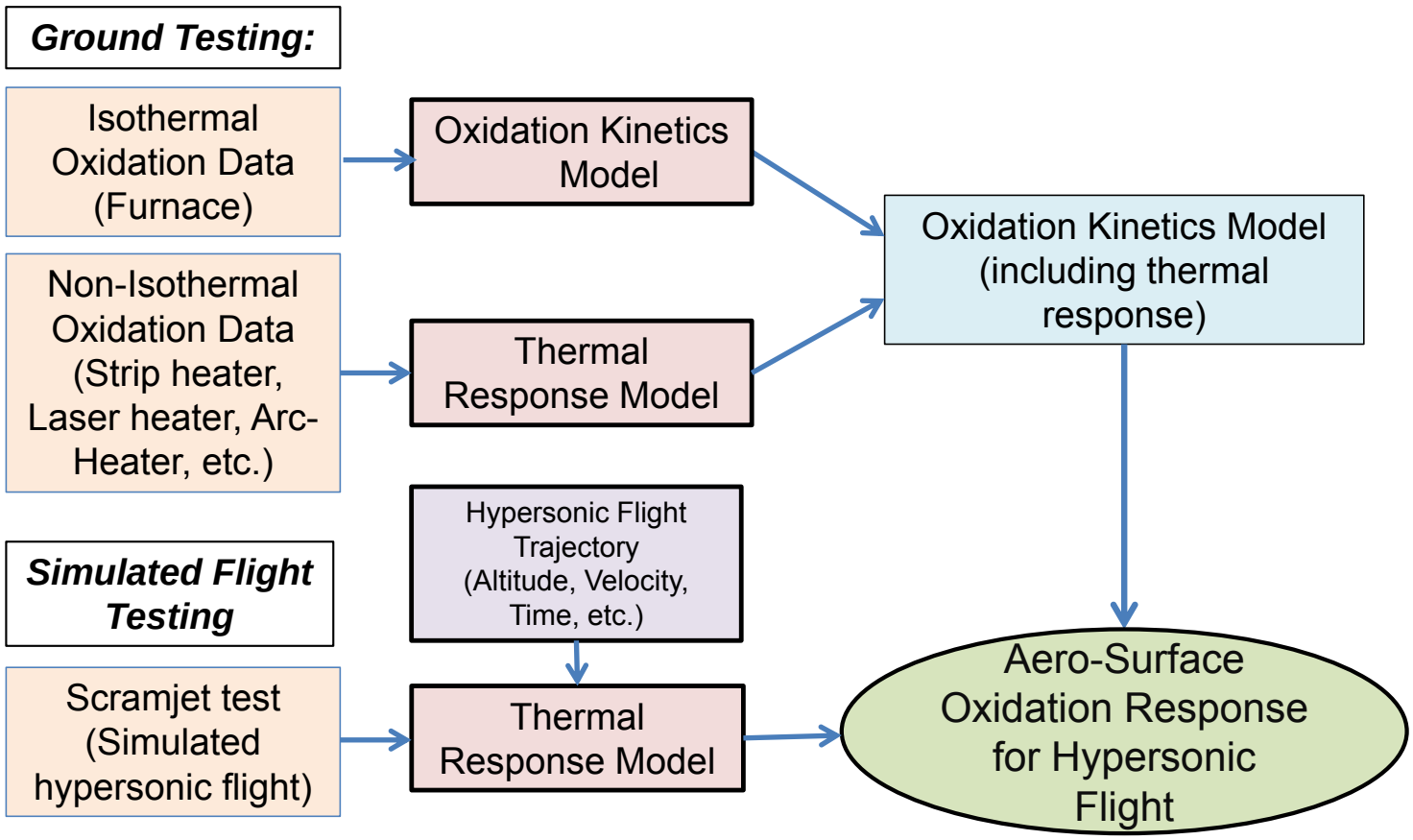

Figure 1

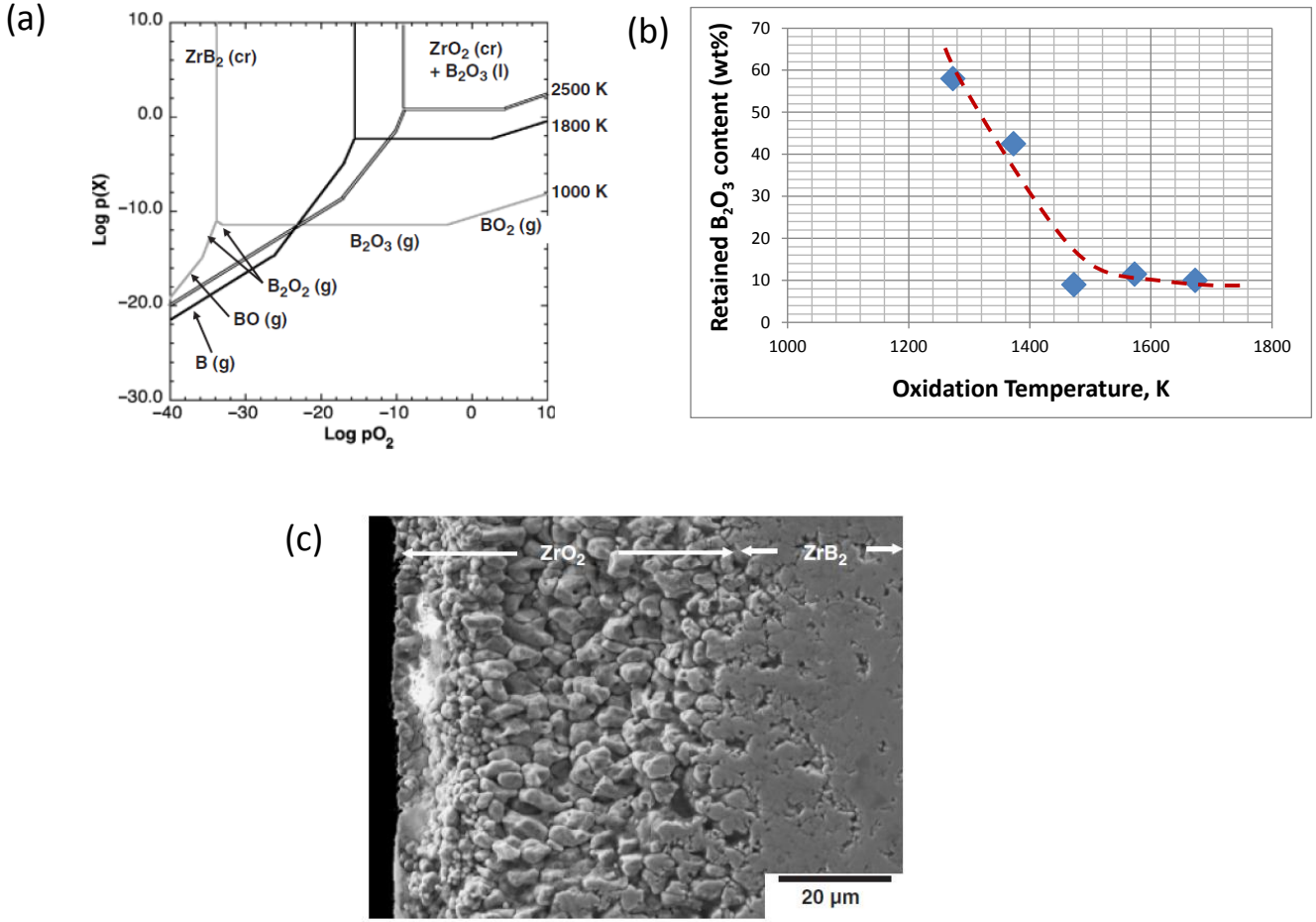

Figure 2

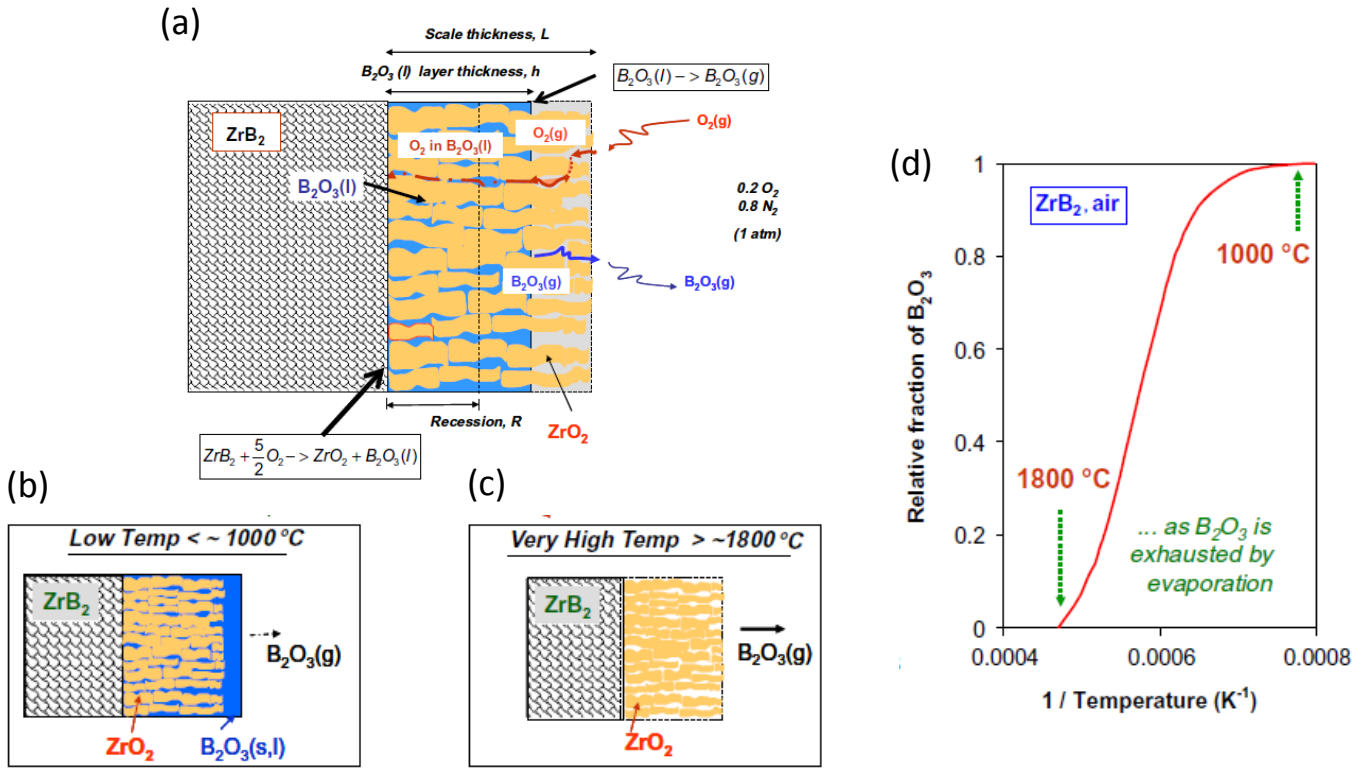

Figure 3

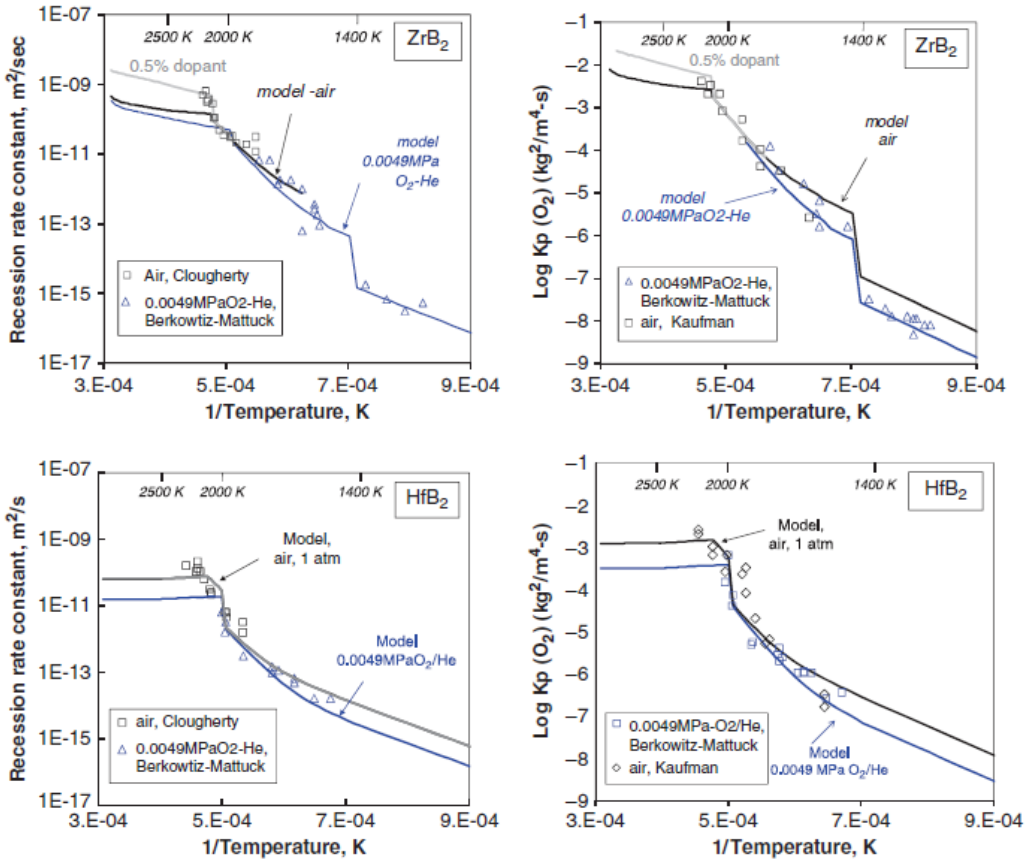

Figure 4

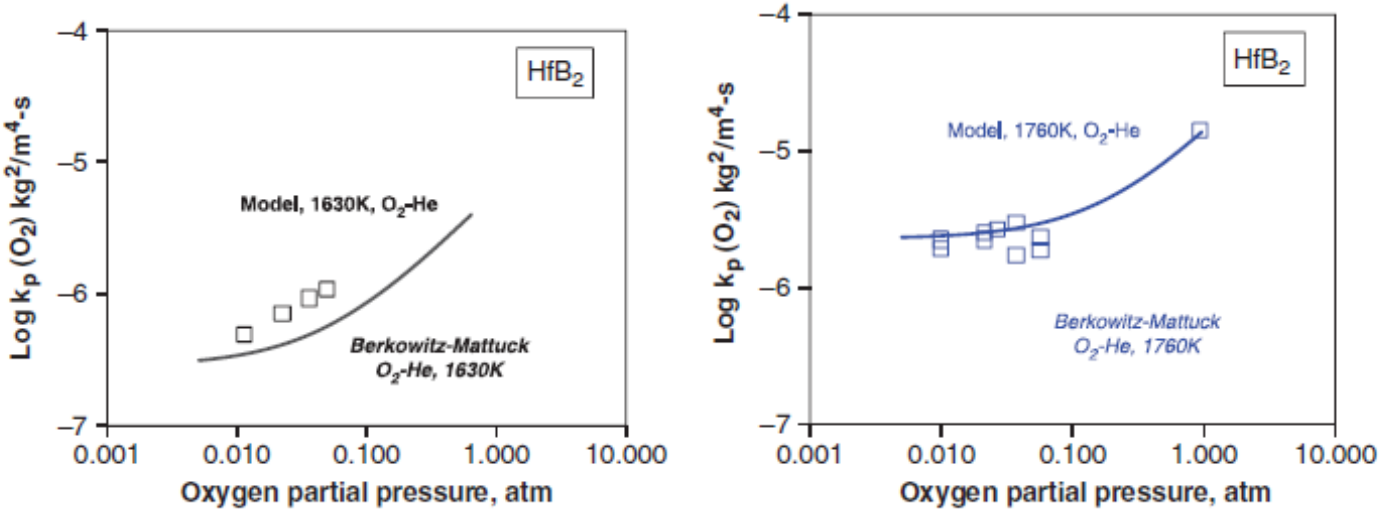

Figure 5

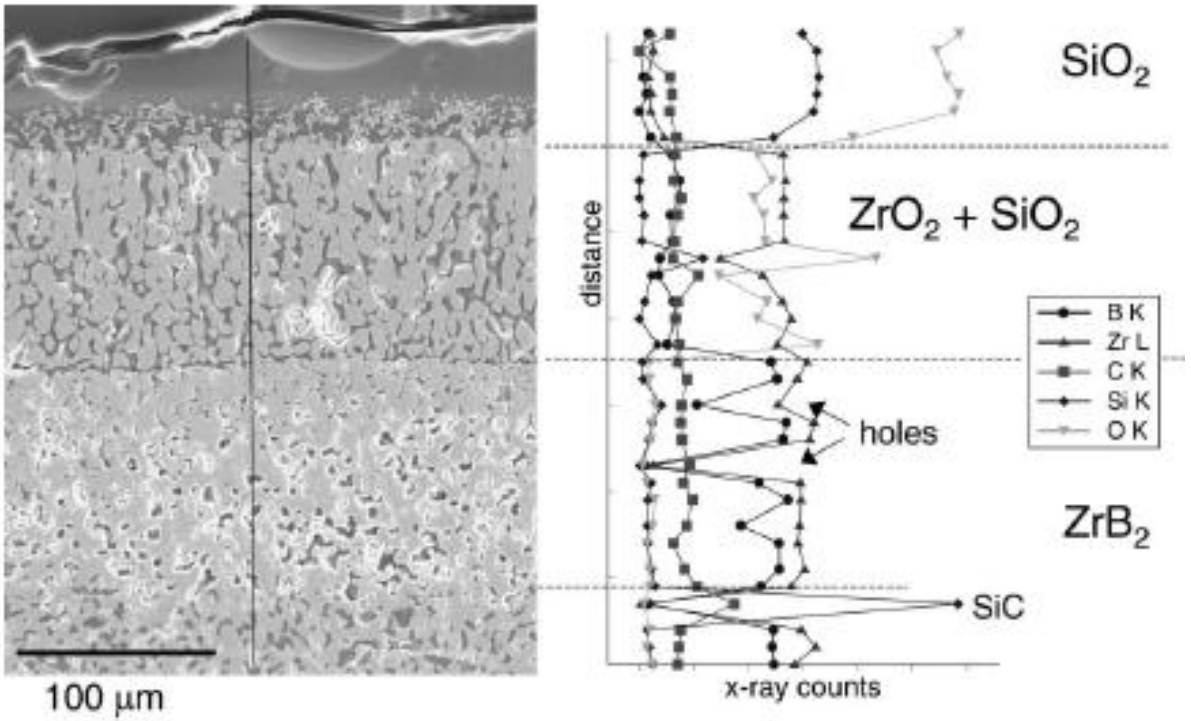

Figure 6

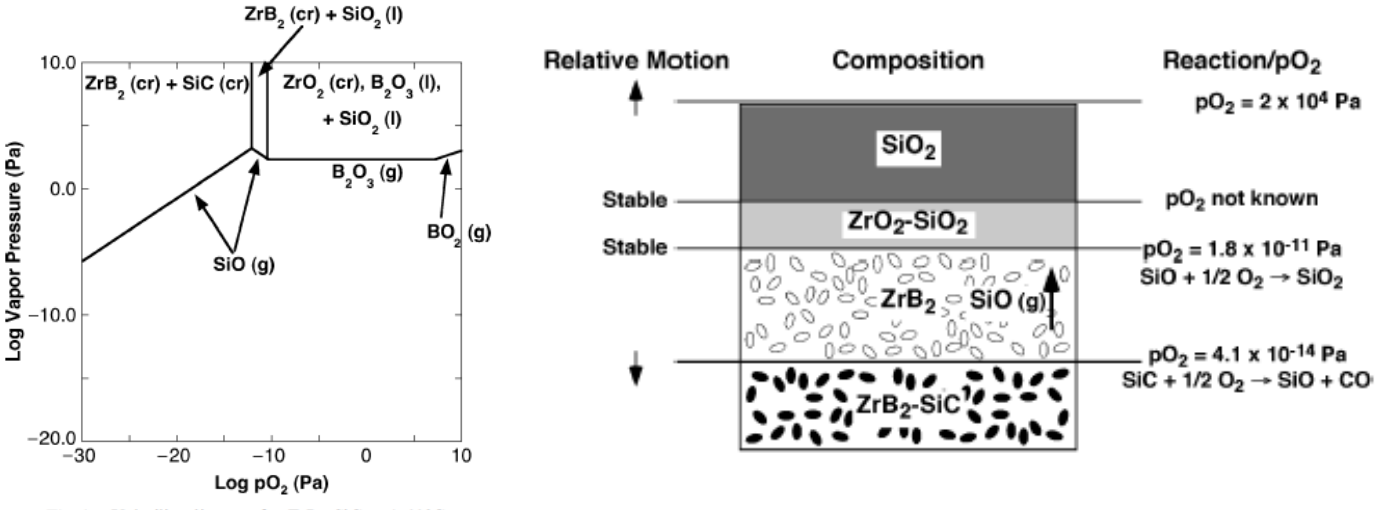

Figure 7

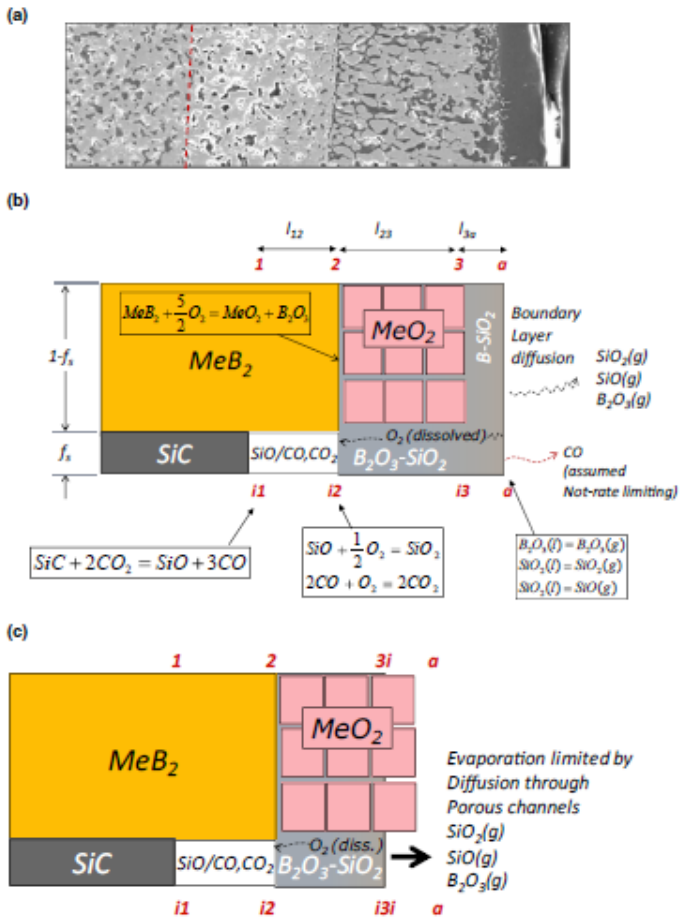

Figure 8

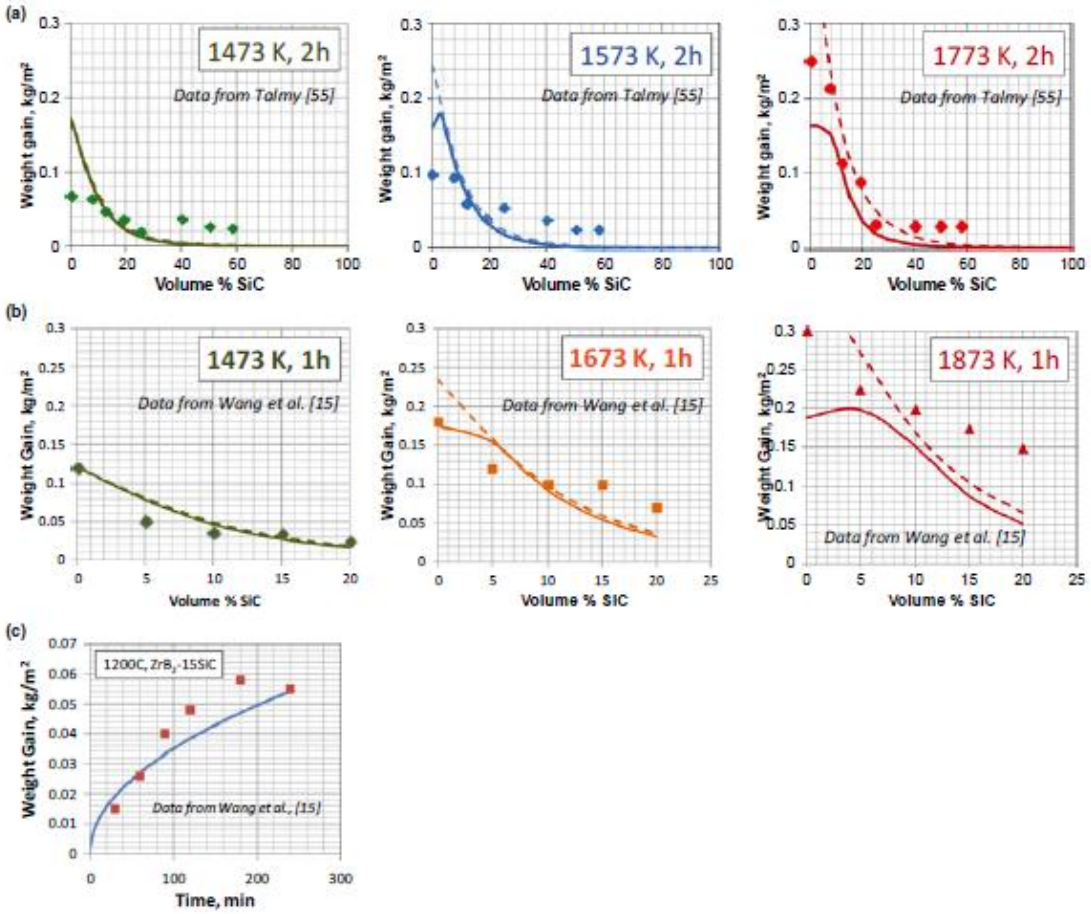

Figure 9

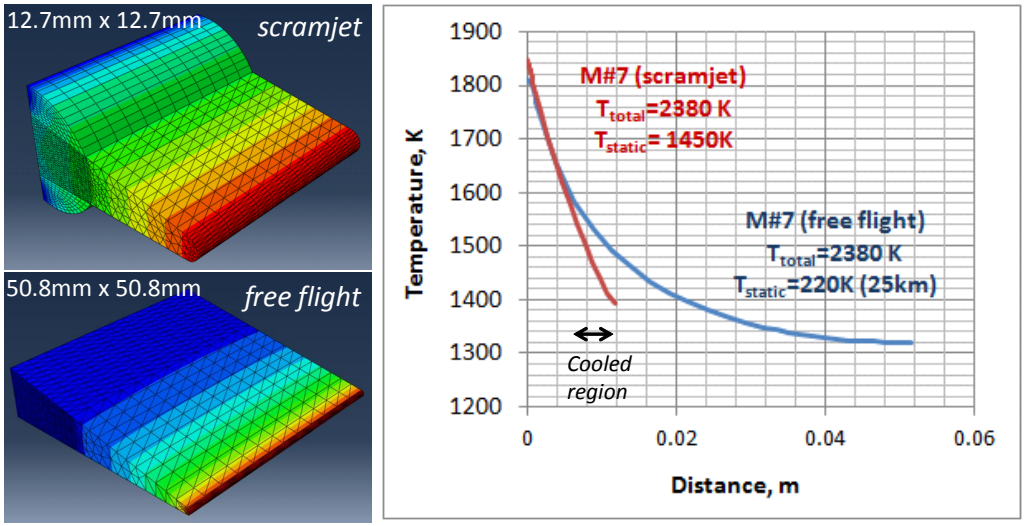

Figure 10

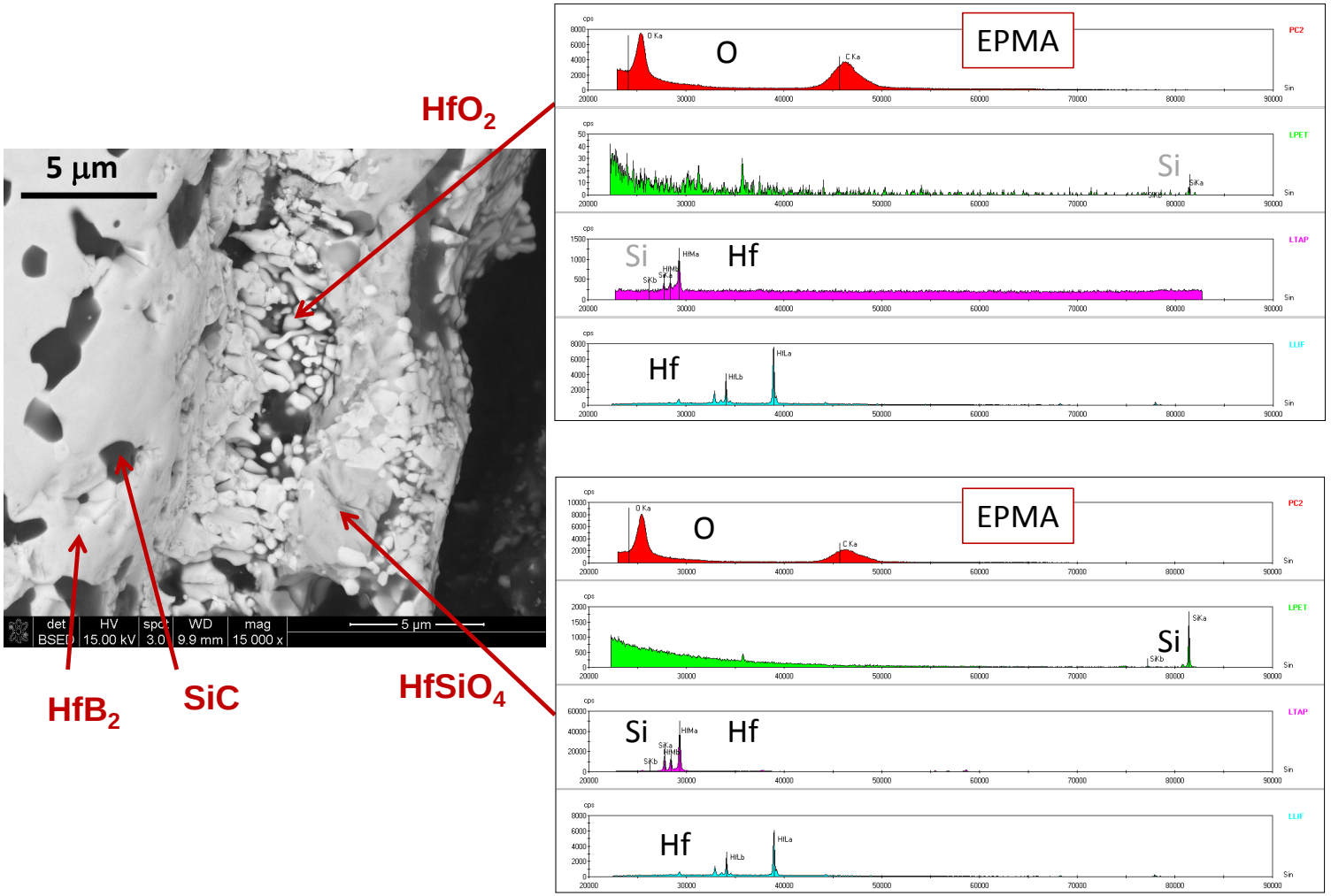

Figure 11

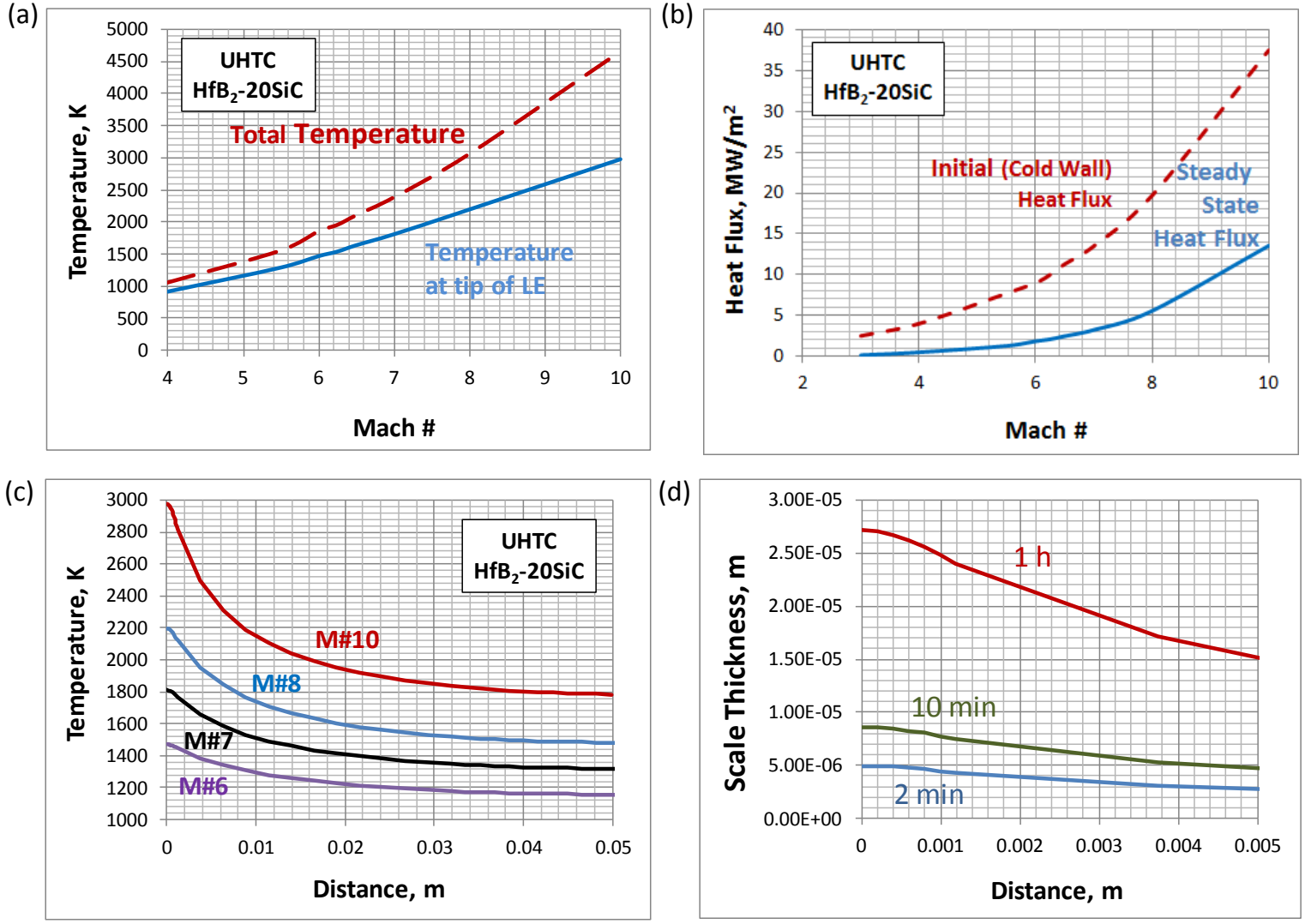

Figure 12